

The WD40-repeat protein Pwp1p associates *in vivo* with 25S ribosomal chromatin in a histone H4 tail-dependent manner

Noriyuki Suka, Emiko Nakashima, Kaori Shinmyozu, Masumi Hidaka and Hisato Jingami*

Department of Molecular Biology, Biomolecular Engineering Research Institute, 6-2-3, Furuedai, Suita, Osaka 565-0874, Japan

Received January 26, 2006; Revised and Accepted June 23, 2006

ABSTRACT

The tails of core histones (H2A, H2B, H3 and H4) are critical for the regulation of chromatin dynamics. Each core histone tail is specifically recognized by various tail binding proteins. Here we screened for budding yeast histone H4-tail binding proteins in a protein differential display approach by two-dimensional gel electrophoresis (2DGE). To obtain highly enriched chromatin proteins, we used a Mg^{2+} -dependent chromatin oligomerization technique. The Mg^{2+} -dependent oligomerized chromatin from H4-tail deleted cells was compared with that from wild-type cells. We used mass spectrometry to identify 22 candidate proteins whose amounts were reduced in the oligomerized chromatin from the H4-tail deleted cells. A *Saccharomyces* Genome Database search revealed 10 protein complexes, each of which contained more than two candidate proteins. Interestingly, 7 out of the 10 complexes have the potential to associate with the H4-tail. We obtained *in vivo* evidence, by a chromatin immunoprecipitation assay, that one of the candidate proteins, Pwp1p, associates with the 25S ribosomal DNA (rDNA) chromatin in an H4-tail-dependent manner. We propose that the complex containing Pwp1p regulates the transcription of rDNA. Our results demonstrate that the protein differential display approach by 2DGE, using a histone-tail mutant, is a powerful method to identify histone-tail binding proteins.

INTRODUCTION

A nucleosome comprises ~200 bp of DNA, an octameric core of two copies each of histones H2A, H2B, H3 and H4, and the linker histone H1. The core histone proteins contain histone-fold domains and histone-fold extensions responsible for histone–histone and histone–DNA interactions, and N-terminal tail domains. The crystal structure of the nucleosome core particle revealed that the N-terminal tails are predominantly external to the particle and highly flexible, suggesting that they interact with DNA/histones, and also serve as targets for chromatin binding proteins and enzymatic functions (1). Consistent with the idea that the histone-tails mediate the key nucleosome–nucleosome interactions that are essential for chromatin structures *in vivo*, the histone-tails were shown to be critical for both the intramolecular folding of nucleosomal arrays and the fiber–fiber interactions observed *in vitro* (2). The locations and interactions of the H3 tail domain are dependent upon the degree of the condensation of a nucleosomal array, and alterations in the tail-interactions may elaborate different structural and functional states of chromatin (3). Thus, the core histone tail domains are essential determinants of chromatin fiber dynamics. In the chromatin context *in vivo*, the tails electrostatically interact with DNA. In addition, histone tails also interact with other tails, other histone domains and non-histone proteins.

The histone-tail-binding proteins associate with specifically modified tails and induce various chromatin functions. In yeast, repressor proteins, such as Sir3p, and transcriptional activators, such as the bromodomain-containing protein Bdf1p, interact with the histone H4 tail (4–7). The N-terminal tail of histone H4 has four acetylated lysines: K5, K8, K12 and K16. Of these, only K16 is strongly correlated with a specific regulatory function in yeast, where its acetylation state

*To whom correspondence should be addressed at Office of Graduate Courses for Integrated Research Training, Kyoto University Faculty of Medicine, Sakyo-Ku, Kyoto 606-8501, Japan. Tel: +81 75 753 9493; Fax: +81 75 753 9495; Email: jingami@four.med.kyoto-u.ac.jp
Present addresses:

Noriyuki Suka, Protein Research Group, Protein Structure Team, RIKEN GSC, Yokohama 230-0045, Japan

Kaori Shinmyozu, Laboratory for Germline Development, Center for Developmental Biology, RIKEN Kobe Institute, Kobe 650-0047, Japan
Masumi Hidaka, Medical Biophysics and Radiation Biology, Faculty of Medical Science, Kyushu University, Fukuoka 812-8582, Japan

regulates the extent of heterochromatin silencing. K16 is acetylated by Sas2p and deacetylated by Sir2p, and the balance of these opposing activities determines the extent of silencing spreading from telomeres (8,9). The spreading is in part owing to Sir3p's preferential association with the H4-tails that have been deacetylated at K16. In contrast, Bdf1p preferentially associates with acetylated H4-tails. Bdf1p competes with a Sir2p deacetylase for binding to the acetylated H4-tails (7). Besides acetylation, methylated H3-tails are recognized by repressor proteins, such as heterochromatin protein 1 (HP1) and Polycomb, in higher eukaryotes (10–12). The chromodomains of HP1 and Polycomb associate with H3-tails methylated at K9 and K27, respectively, leading to changes in DNA template accessibility and higher-order chromatin structures.

The molecular interaction partners of the histone tails in different states of modification are being elucidated and have been shown to play key roles in the regulation of all nuclear processes, leading to an 'epigenetic code' or 'histone code' hypothesis (13). Based on this hypothesis, histone-tail-binding proteins have been isolated by affinity columns using histone tail peptides with specific modifications. This approach identified various factors, such as a nucleosome remodeling and deacetylase (NuRD) complex, hSNF2H, an inhibitor of acetyltransferase (INHAT) complex, a WD40-repeat protein WDR5, and 14-3-3 isoforms of phosphospecific binding proteins as H3-tail-binding proteins (14–18). These identifications indicated that the peptide columns are a powerful approach to screen for the tail-binding proteins. However, the screening is probably biased, since the binding to the peptides is performed *in vitro*. Thus, many tail-binding proteins may still be unidentified. Therefore, it is worthwhile to perform the screening for the tail-binding proteins by *in vivo* binding.

Here we screened for potential histone H4-tail associated proteins using a protein differential display approach by two-dimensional gel electrophoresis (2DGE) comparing H4 tail deleted chromatin with wild-type chromatin. We have found that a WD40-repeat protein, Pwp1p, interacts with chromatin through the H4-tail, which confirms that our approach is effective for identifying histone-tail-associated proteins.

MATERIALS AND METHODS

Yeast strains, genetic techniques and media

The strains used in this study were a wild type strain (WT), ENY012 [isogenic with PKY501 (19) except for SIR3-FLAG], a histone H4 N-terminal tail (amino acids 4–28) deleted strain (H4-tail Δ), ENY017 [isogenic with PKY813 (19) except for SIR3-FLAG], ENY091 (isogenic with PKY501 except for TAF14-FLAG and PWP1-Myc), ENY092 (isogenic with PKY813 except for TAF14-FLAG and PWP1-Myc), ENY098 (isogenic with PKY501 except for PWP1-FLAG), and ENY102 (isogenic with PKY813 except for PWP1-FLAG). The tags were fused to the genes with a PCR-based one-step *in vivo* tagging strategy, using the FLAG tag vector p3FLAG-KanMX (20) and pFA6a-13Myc-TRP1 (21). Transformations of yeast strains were performed by the lithium chloride method. Transformed

cells were plated onto YPD plates containing 200 μ g/ml of G418 disulfate (Nacalai Tesque) or synthetic medium plates lacking tryptophan. Integration of the tag-encoding DNA was confirmed by PCR, followed by western blot analyses with anti-FLAG M2 (Sigma) and anti-Myc-tag monoclonal antibodies (Cell Signaling Technology, 9B11, #2276).

Preparation of MNase eluted chromatin

Yeast cells were grown in 200 ml of YPD medium at 30°C to an A₆₀₀ of \sim 1.0. Cells were spheroplasted according to Liang and Stillman (22), with some modifications. Cells were incubated at room temperature for 5 min in 2 ml of pre-spheroplasting buffer [100 mM PIPES (pH 9.4) and 10 mM DTT], followed by an incubation in 2 ml of spheroplasting buffer [50 mM KH₂PO₄/K₂HPO₄ (pH 7.5), 0.6 M sorbitol and 10 mM DTT] containing either 2 mg/ml (for wild-type strain) or 6 mg/ml (for tail deleted strain) of Yeast Lytic Enzyme (ICN) at room temperature for 10 min with occasional mixing, until the OD₆₀₀ of a 1:100 dilution of the cell suspension (in water) dropped to <25% of the value before digestion. Spheroplasts were washed with 2 ml of ice-chilled wash buffer [100 mM KCl, 50 mM HEPES-KOH (pH 7.5), 2.5 mM MgCl₂ and 0.4 M sorbitol], and then were pelleted at 3000 r.p.m. for 5 min in a microcentrifuge at 4°C. Crude cell nuclei were prepared from the spheroplasts according to Alfieri and Clark (23), with some modifications. The spheroplasts were lysed by vigorous resuspension with a pipette in 2 ml of spheroplast lysis buffer 18% (wt/vol) Ficoll 400, 0.2% Triton X-100, 40 mM potassium phosphate (pH 7.5), 2 mM Na-EDTA, 0.5 mM Na-EGTA, 0.5 mM spermidine hydrochloride, 0.15 mM spermine hydrochloride, 10 mM 2-ME and Complete protease inhibitor cocktail (Roche)]. The lysate was layered over 4 ml of a sucrose step gradient [65% (wt/vol) sucrose, 40 mM potassium phosphate (pH 7.5), 2 mM Na-EDTA, 0.5 mM Na-EGTA, 0.5 mM spermidine hydrochloride, 0.15 mM spermine hydrochloride, 10 mM 2-ME and Complete protease inhibitor cocktail (Roche)] and spun at 14 000 r.p.m. for 30 min in a microcentrifuge at 4°C. The nuclear pellet was resuspended in 0.8 ml of nuclei lysis buffer [50 mM Tris-HCl (pH 8.0), 5 mM Na-EDTA, 5 mM 2-ME and Complete protease inhibitor cocktail (Roche)]. RNase (32 μ l, DNase free, 10 mg/ml) was added, and after incubating for 30 min on ice, the mixture was spun at 10 000 r.p.m. for 3 min at 4°C. This step of the nuclear lysis was repeated once. The lysed nuclei were resuspended in 1 ml of MN buffer [10 mM Tris-HCl (pH 8.5) and 2 mM CaCl₂], kept on ice for 15 min, and spun at 10 000 r.p.m. for 3 min at 4°C. This washing step with the MN buffer was repeated once. The lysed nuclei were resuspended in 1 ml of MN buffer again, and were incubated at room temperature for 5 min. Micrococcal nuclease (MNase) (5 μ l, 10 000 U/ml, Worthington) was added. The digestion was performed for 1 min at room temperature, stopped by adding 30 μ l of 100 mM EGTA and cooled on ice for 15 min. The supernatant was recovered by centrifugation at 10 000 r.p.m. for 3 min at 4°C. The lysed nuclei pellet was resuspended in 0.5 ml MN buffer with 3 mM EGTA and kept on ice for 15 min. The supernatant was recovered by centrifugation at 10 000 r.p.m. for 3 min at 4°C and was combined with the

first supernatant (MNase eluted chromatin). Western blot analyses were performed with anti-H3 histone (Abcam, ab1791), anti-H2A histone (Abcam, ab4075), anti-H4 histone (Cell Signaling Technology, #2592), anti-BDF1 (gift from S. Roeder), anti-PGK1 (Molecular Probes, A-6457), anti-FLAG (Sigma) and anti-Myc antibodies (Cell Signaling Technology, 9B11, #2276) by an ECL Plus detection system (Amersham). The detection and quantitation of the signals were performed by a lumino-imager (LAS-1000plus, Fujifilm). Purified histones were purchased from Sigma (type II-A from calf thymus).

Oligomerization of MNase eluted chromatin by Mg^{2+} ions

The MNase eluted chromatin was chilled on ice for 15 min, and after centrifugation at 15 000 r.p.m. for 15 min in a microcentrifuge, the supernatant was recovered. A $MgCl_2$ solution was added to 12 mM, and after chilling on ice for 15 min, the mixture was spun at 15 000 r.p.m. for 15 min. The oligomerized chromatin was recovered in the precipitate. In Figure 2A, the $MgCl_2$ solution was added to achieve the desired final salt concentration. The DNA was purified, electrophoresed on a 2% agarose gel and stained with ethidium bromide.

2DGE and protein identifications by mass spectrometry (MS)

The oligomerized chromatin (30–50 μ g) was dissolved in 125 μ l of rehydration buffer [7 M urea, 2 M thiourea, 4% CHAPS, 0.1% bromophenol blue, 0.5% IPG buffer (Amersham) and 1.5 μ l DeStreak Reagent (Amersham)] and applied to 7 cm isoelectric focusing (IEF) strips (Amersham Immobilin DryStrip pH 3–10 NL, 7cm). Strip rehydration and IEF were performed in an Ettan IPGphor II isoelectric focusing system (Amersham) according to the manufacturer's manual. The focused strips were used immediately for the second dimension. The second dimension was performed on a NuPAGE 4–12% Bis–Tris ZOOM Gel (Invitrogen), according to the manufacturer's recommendations. Gels were stained with a Silver Stain MS kit (Wako Pure Chemical). Selected protein spots were excised and in-gel digested with trypsin. The peptides extracted from the gels were separated on a PepMap C18 (75 μ m \times 15 cm, LC Packings) column using a capillary HPLC and directly applied to a Micromass hybrid quadrupole time-of-flight (Q-ToF micro) mass spectrometer (Micromass, Manchester, UK). Data derived from the MS/MS spectra were used to search the NCBI non-redundant protein database with the Mascot program (Matrix Science).

Chromatin immunoprecipitation

Chromatin immunoprecipitation (ChIP) and PCR were performed as described previously (24,25), with some modifications. Immunoprecipitation of Pwp1p-FLAG or Sir3p-FLAG was done in FA lysis buffer containing 20 mM $NaCl_2$ with 25 μ l of anti-FLAG M2-agarose beads (50% slurry, Sigma) for 125 μ l of whole cell extract. The immunoprecipitate was washed three times in the same buffer, and the elution was done by the addition of FLAG peptide (Sigma) to

200 μ g/ml. PCR was performed with a 1/250 portion of immunoprecipitated DNA within a linear range of amplification. The linear range of amplification was confirmed by serial 2.5-fold dilutions of an input DNA as templates (Figure 6A and 6C). The products were electrophoresed on a 6% polyacrylamide gel and were stained with SYBR Gold (Invitrogen). The signals of the PCR products were quantified with a fluoro-imager (LAS-1000plus, Fujifilm). To calculate the relative fold enrichment of Pwp1p or Sir3p binding, we first normalized each signal to the loading control of *CUP1*, and then normalized the signal to an input DNA. The primer sequences used in this study are available upon request.

RESULTS

Preparation of chromatin by MNase digestion

Yeast cells were treated with a lytic enzyme to remove their cell walls and were converted to spheroplasts. The spheroplasts were lysed using Ficoll and Triton X-100, and the cell nuclei were precipitated by centrifugation. The nuclei were lysed by resuspension in a low ionic strength buffer. The genomic chromatin was undamaged and still attached to the nuclear structures. The nuclear pellet still contained some ribosomes, which co-sedimented with the nuclei (23). RNase was used to remove the ribosomes and RNA from the lysed nuclei. The genomic chromatin was then released by digestion with MNase from the lysed nuclei (the MNase-eluted chromatin fraction) (Figure 1A). As shown in Figure 1B, we detected nucleosomal ladders with the MNase digestion, indicating that soluble chromatin was eluted from the purified nuclei by the MNase digestion. Without MNase, no nucleosomal ladder was detected, indicating that no chromatin was eluted from the nuclei. We also confirmed the equal elution of chromatin at different genomic regions by quantitating the amounts of DNA at selected heterochromatin and euchromatin regions (data not shown).

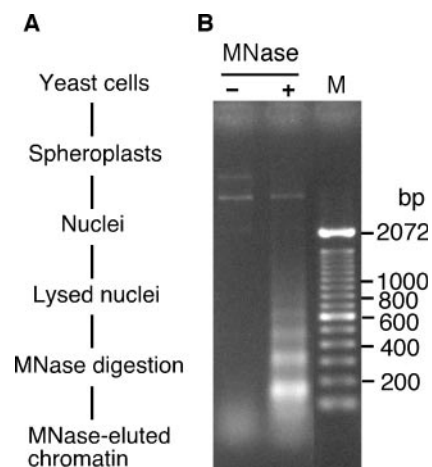


Figure 1. Preparation of MNase-eluted chromatin. (A) The biochemical fractionation scheme. (B) DNA from the MNase-eluted chromatin fraction, either with (+) or without (–) the MNase digestion, was electrophoresed on a 2% agarose gel and visualized by ethidium bromide staining. M is DNA size markers.

Evaluation of chromatin fractionation by Mg^{2+} -dependent oligomerization

MNase digestion of chromatin may also cause the release of non-chromatin associated proteins from the nuclei. Therefore, proteins that are not associated with chromatin may be included in the MNase-eluted chromatin fraction. These contaminating proteins should be removed for effective screening of the chromatin-associated proteins.

Chromatin condenses and oligomerizes in the presence of Mg^{2+} ions. This property is called Mg^{2+} -dependent oligomerization (2,26). The addition of increasing concentrations of Mg^{2+} ions to an unfolded array of nucleosomes in a low salt buffer causes a series of conformational changes and leads to the formation of a highly folded state. In addition to the intra-fiber conformational changes, inter-fiber-interactions also occur, resulting in the oligomerization between the fibers. The oligomerized chromatin is easily precipitated by centrifugation. We investigated whether the Mg^{2+} -dependent oligomerization of the MNase-eluted chromatin separates the chromatin-associated proteins from the non-associated proteins. As shown in Figure 2A, a Mg^{2+} ion titration was conducted. After the addition of various Mg^{2+} ion concentrations and centrifugation, the DNA was purified from both the supernatant and precipitate, fractionated on an agarose gel, and visualized by ethidium bromide staining. A larger amount of DNA was precipitated with higher concentrations of the Mg^{2+} ions. We found that most of the chromatin was oligomerized and fractionated into the precipitate with 12 mM Mg^{2+} ions. We used this concentration for our preparation of the oligomerized chromatin fraction.

We next analyzed the proteins in the supernatant and the precipitate produced by the fractionation with the 12 mM Mg^{2+} ions. The proteins in both fractions were detected by silver staining. Most of the DNA was in the precipitate, as described above. In contrast, about a half of the proteins

remained in the supernatant (Figure 2B). We speculated that the proteins in the supernatant would not be associated with the chromatin because they did not fractionate into the precipitate, where most of the DNA fractionated. This speculation is supported by the observation of the distinct composition of each fraction. For example, core histones, fundamental chromatin components, were fractionated into the precipitate and became major bands in the precipitate, as identified with histone markers. Lower amounts of histones were present in the supernatant, which was consistent with less DNA in the supernatant. On the other hand, protein bands between 37 and 75 kDa were abundant in the supernatant. This suggests that chromatin and its associated proteins, but not proteins that do not associate with chromatin, were specifically fractionated into the precipitate by the chromatin oligomerization.

To confirm our speculation, we performed a western blot analysis (Figure 2C). Histones H2A, H3 and H4 were detected in the precipitate but not in the supernatant, confirming the result from the silver stain. Together with the DNA distribution described above, this indicates that basic components of chromatin, such as DNA and core histones, are precipitated by the Mg^{2+} -dependent oligomerization. To investigate whether non-histone chromatin proteins are also present in the precipitate, we analyzed Sir3p and Bdf1p. A western blot analysis revealed that both Sir3p and Bdf1p were present only in the precipitate. This result suggests that the non-histone chromatin proteins, in addition to the basic chromatin components, also fractionated into the precipitate. Finally, we assessed the distribution of an abundant cytoplasmic marker protein, Pgc1p. In contrast to the chromatin proteins analyzed above, we detected Pgc1p only in the supernatant. This indicates that Pgc1p contaminated the MNase-eluted fraction, but was excluded by the Mg^{2+} -dependent oligomerization, and suggests that the non-chromatin associated proteins are

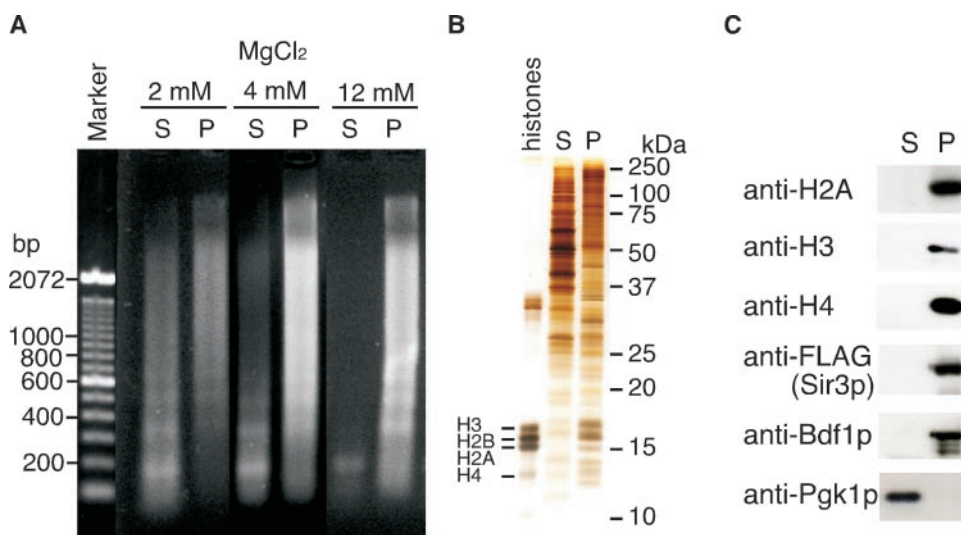


Figure 2. Fractionation of the MNase-eluted chromatin by the Mg^{2+} -dependent oligomerization. (A) Titration of the Mg^{2+} concentration. The DNAs fractionated by various concentrations of Mg^{2+} , in the supernatant (S) and precipitate (P), were electrophoresed on a 2% agarose gel and were visualized by ethidium bromide staining. (B) The protein compositions of the fractions (S and P) by the Mg^{2+} -dependent oligomerization with 12 mM Mg^{2+} . The fractionated proteins and purified histones were resolved by SDS-PAGE and were visualized by silver staining. Molecular weight markers are indicated. (C) The distribution of the proteins fractionated as shown in (B) were analyzed by western blot analyses with the antibodies indicated on the left.

not precipitated by the Mg^{2+} ions. We concluded that the oligomerized chromatin fractionation by the Mg^{2+} ions is useful to isolate the chromatin proteins.

The oligomerized chromatin from H4-tail deleted cells

We assumed that the H4-tail associated-proteins would be absent from the chromatin lacking the H4-tails. We compared the proteins of the oligomerized chromatin from the H4-tail Δ with those from the WT. Silver stained gels revealed that about equal amounts of H3, H2A and H2B were present in both oligomerized chromatin fractions (Figure 3A). In the H4-tail deleted chromatin, a band corresponding to the tail-deleted H4 (indicated as H4 Δ on the left in Figure 3A) was present instead of the wild-type H4 band and was detected by western blotting with an anti-H4 antibody against the C-termini of histone H4 (data not shown). We further analyzed histones H2A and H3 by western blotting (Figure 3B), and observed equal amounts of H2A and H3 in the oligomerized chromatin fractions from both cells.

To elucidate whether our strategy would be useful for identifying H4-tail associated proteins, we again analyzed Sir3p and Bdf1p, which both interact with the H4-tails (4–7). Although the total amount of either Sir3p or Bdf1p in each strain was not changed (data not shown), lower amounts of both proteins were present in the oligomerized chromatin of the H4-tail deleted cells (Figure 3B compare WT and H4-tail Δ). This suggests that the amounts of H4 tail-binding proteins, such as Sir3p and Bdf1p, are decreased

in the oligomerized chromatin fraction prepared from the H4 tail-deleted cells.

Identification of the candidate proteins that associate with the H4-tail

The proteins associated with the oligomerized chromatin from the WT and H4-tail Δ strains were then resolved by 2DGE and visualized by silver staining (Figure 4). The amount of the chromatin was measured by western blot analysis with the anti-H3 antibody, and then equal amounts of the oligomerized chromatin from the WT and H4-tail Δ strains were applied to the 2D gels. Over 350 protein spots were detected. We selected 36 spots representing proteins whose amounts were reduced in the fraction from H4-tail deleted cells. A total of 39 proteins were identified by the MS from the 36 spots (Figure 4).

We excluded the predicted contaminating proteins (Figure 4 in gray), which appeared non-specifically in previously reported large-scale experiments of protein complexes (27–29), from the 39 identified proteins. The predicted contaminants are abundant proteins in the cell, such as a ribosomal protein, a chaperone protein, and a metabolic enzyme. We also subtracted yeast transposons and L-A virus proteins. Consequently, we found 22 proteins whose amounts were reduced in the oligomerized chromatin fraction of the H4-tail Δ , as candidates for the H4 tail-associated proteins (Table 1). The steady state transcription levels of the genes that encode these 22 proteins did not significantly differ between the WT and H4-tail Δ strains (data not shown). The largest change was a 1.82-fold decrease in *FPR4* expression. This suggests that the observed reduction in the amount of the proteins is not owing to a reduction of the gene expression.

Of the 22 potential proteins, two proteins, Arp4p and Isw1p, have already been shown to be involved in chromatin regulation via the H4 tail, and five proteins, Isw1p, Rsc8p, Pwp1p, Tif34p and YDL156p, contain a possible histone-tail-binding domain (SANT or WD40-repeat). Therefore, it is likely that our candidates are histone H4-tail-associated proteins. The interaction between Arp4p and histone-tails is supposed to contribute to the recruitment of an Arp4p-containing nucleosome acetyltransferase of histone H4 (NuA4) complex to nucleosomes (30,31). Isw1p, one of yeast imitation switch (ISWI) homologs, requires the H4-tail for its chromatin remodeling activity. ISWI probably recognizes a DNA-bound H4-tail, as a patch of three residues, R17H18R19, that contact nucleosomal DNA, to stimulate the ATPase activity (32). Isw1p and Rsc8p contain a SANT domain, which was identified based on its homology to the DNA binding domain of c-Myb and is also present in the SWI3, ADA2, nuclear receptor co-repressor N-CoR and transcription factor (TF)IIIB factors, and is envisaged as a histone-tail-binding module that regulates the chromatin remodeling activity of the associated complex (33). Pwp1p, Tif34 and YDL156Wp have a WD40-repeat domain, which functions in the interactions among proteins in many cellular complexes including chromatin-regulated proteins. Several chromatin-regulated proteins containing the WD40-repeat are known as histone-tail binding proteins (described in Discussion). More interestingly, a WD40-repeat of WDR5 was shown to interact with histone H3-tails (17).

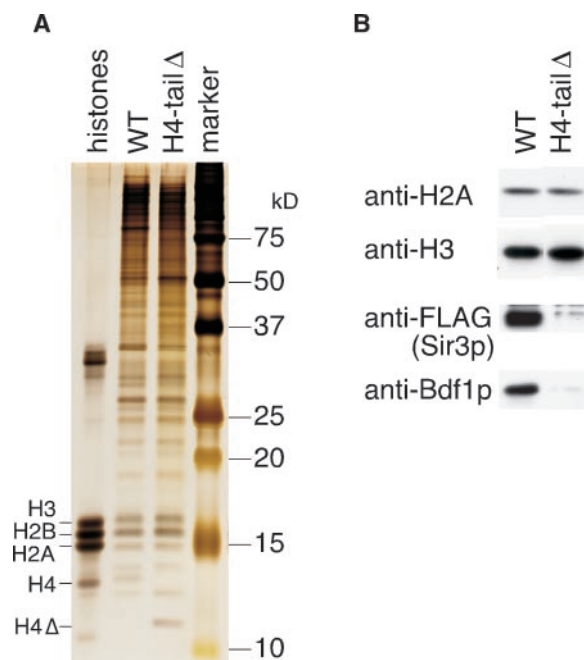


Figure 3. Comparison of the oligomerized chromatin fractions between WT and H4-tail Δ . (A) The oligomerized chromatin proteins from the WT and H4-tail Δ strains were resolved by 15% SDS-PAGE and were visualized by silver staining. Purified histones were run and the position of each core histone is indicated on the left. Molecular weight markers are indicated on the right. (B) Western blot analyses of oligomerized chromatin proteins from the WT and H4-tail Δ strains. Histones (H2A and H3) and tail binding proteins (Sir3p and Bdf1p) in each oligomerized chromatin fraction (WT and H4-tail Δ) were analyzed with the antibodies indicated on the left.

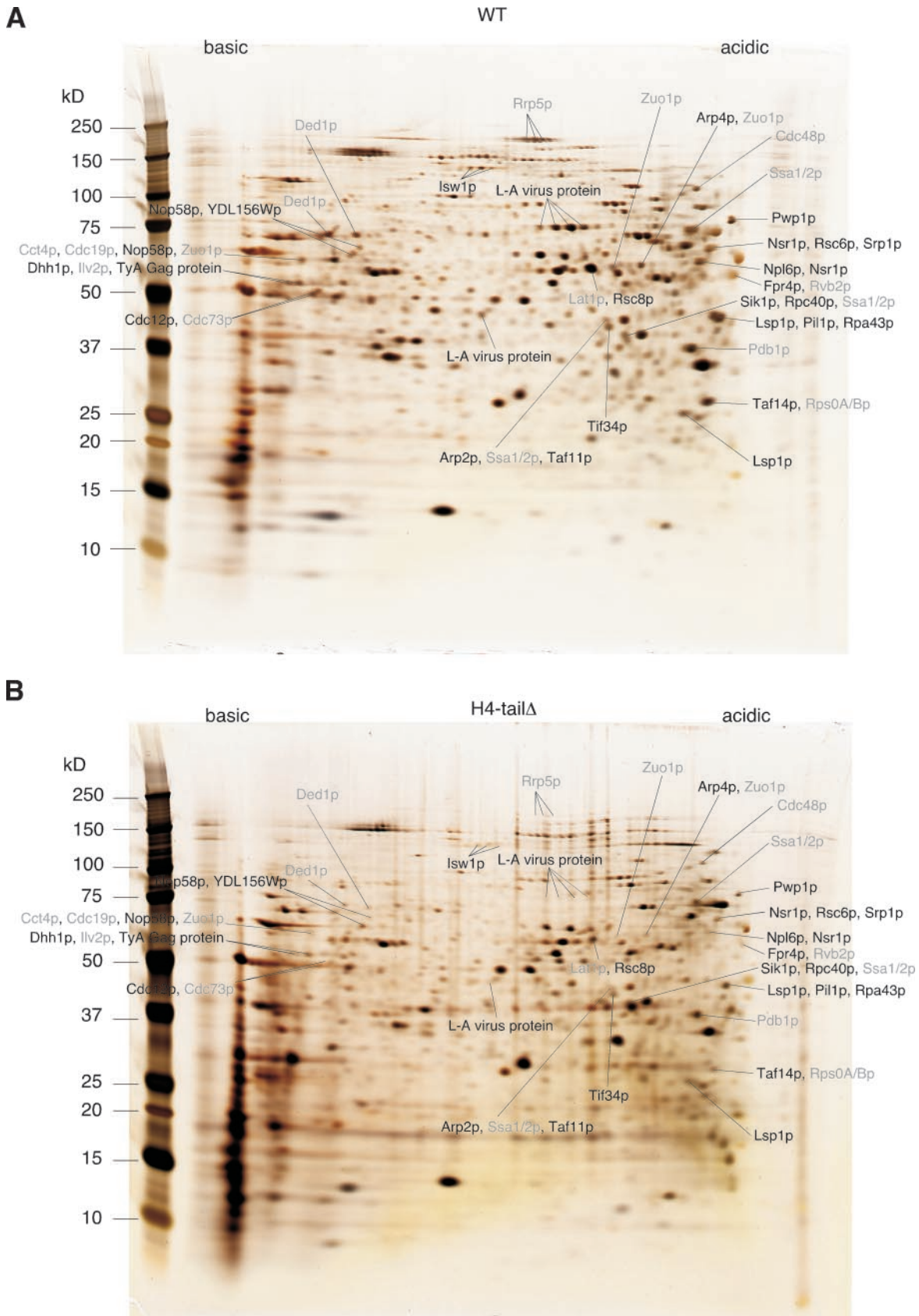


Figure 4. The protein differential display approach of the oligomerized chromatin proteins by 2DGE. The oligomerized chromatin fractions from WT (A) and H4-tail Δ (B) cells were resolved by 2DGE and visualized by silver staining. The protein spots with signal intensity that was reduced in the H4 tail-deletion are indicated and were identified by MS. Predicted contaminant proteins are shown in gray.

Table 1. Candidate proteins that associate with chromatin by H4-tail

Protein	Domain	Description ^a
Arp2p		Actin-related protein, essential component of the Arp2/3 complex
Arp4p		Nuclear actin-related protein involved in chromatin remodeling
Cdc12p		Component of the septin ring of the mother-bud neck that is required for cytokinesis
Dhh1p		Cytoplasmic DEXD/H-box helicase may have a role in mRNA export and translation
Fpr4p		Nuclear protein, putative peptidyl-prolyl <i>cis</i> - <i>trans</i> isomerase
Isw1p	SANT	Member of the ISWI class of ATP-dependent chromatin remodeling complexes
Lsp1p		Long chain base-responsive inhibitor of protein kinases Phk1p and Phk2p, acts along with Pil1p
Nop56p(Sik1p)		Essential evolutionarily-conserved nucleolar protein component of the box C/D snoRNP complexes
Nop58p		Protein involved in pre-rRNA processing, 18S rRNA synthesis and snoRNA synthesis
Npl6p		Nuclear protein that may have a role in nuclear protein import
Nsr1p		Nucleolar protein that binds nuclear localization sequences
Pil1p		Long chain base-responsive inhibitor of protein kinases Phk1p and Phk2p, acts along with Lsp1p
Pwp1p	WD40	Protein with WD40 repeats involved in rRNA processing
Rpa43p		RNA polymerase I subunit A43
Rpc40p		RNA polymerase subunit, common to RNA polymerase I and III
Rsc6p		One of 15 subunits of the RSC complex
Rsc8p	SANT	One of 15 subunits of the RSC complex
Srp1(Kap60p)		Karyopherin alpha homolog, forms a dimer with karyopherin beta Kap95p
Taf11p(Taf40p)		TFIID subunit (40 kDa), involved in RNA polymerase II transcription initiation
Taf14p(Anc1p)		Subunit (30 kDa) of TFIID, TFIIF and SWI/SNF complexes
Tif34p	WD40	Subunit of the core complex of translation initiation factor 3(eIF3)
YDL156Wp	WD40	Hypothetical protein

^aDescribed in *Saccharomyces* Genome Database (<http://www.yeastgenome.org/>).

Ten complexes that include more than two candidate proteins

Many proteins form complexes to carry out cellular functions. Chromatin is associated with many complexes. Therefore, a decrease in the association of a protein with chromatin means a decrease in the association of its complex with chromatin. We looked for the complexes that contain the 22 proteins, using the *Saccharomyces* genome database (<http://www.yeastgenome.org/>). We found 10 complexes that contain more than two proteins among the 22 proteins. Each of the 22 proteins was included as one of the subunits of the 10 complexes, except for Cdc12p (Table 2). As described below, most of the complexes are probably involved in chromatin-mediated cellular functions.

Table 2. Candidate complexes that associate with chromatin by the H4-tail

Complex #	Name ^a	Candidate proteins contained
#1	yTAP-C116 ^b (24)	Arp4p Isw1p Npl6p Rpc40p Rsc6p Rsc8p
#2	yTAP-C154 ^b (29)	Dhh1p Rpa43p Rpc40p Rsc8p
#3	Nop58/Sik1 ^c (3)	Sik1p Nop58p Nsr1p
#4	NTG1 complex ^d (10)	Arp2p Rpc40p Tif34p
#5	yTAP-C228 ^b (8)	Fpr4p Pwp1p
#6	yTAP-C152 ^b (35)	Rsc8p YDL156Wp
#7	TFIID (15)	Taf11p Taf14p
#8	NuA4 (12)/ INO80 (11)	Arp4p Taf14p
#9	Arp2/Srp1 ^c	Arp2p Srp1p
#10	PKH1 complex ^d (4)	Lsp1p Pil1p

^aThe number of subunits is in parentheses.

^bA complex in Ref. (27).

^cA complex in Ref. (29).

^dA complex in Ref. (28).

^eThis interaction was shown by a co-immunoprecipitation assay in Ref. (45).

Complex #1: Arp4p, Isw1p, Npl6p, Rpc40p, Rsc6p and Rsc8p are components of the yTAP-C116 complex, which was found in a large-scale identification of yeast multi-protein complexes using tandem-affinity purification (TAP)-epitope-tagging (27). TAP-tagged Isw1p, Isw2p or Hhp10p all yielded the yTAP-C116 complex, containing various components of a chromatin remodeling complex, such as an ISWI complex, a RSC (for remodels the structure of chromatin) complex, an INO80 ATPase complex and a NuA4 histone H4/H2A acetyltransferase complex (34). This suggests that the yTAP-C116 complex may be involved in a chromatin remodeling function. The presence of Arp4p and Isw1p indicates that the yTAP-C116 complex appears to associate with chromatin via an H4-tail.

Complex #2: The yTAP-C154 complex contains many subunits of RNA Polymerases I, II and III and may function in transcription (27). Our candidates, Dhh1p, Rpa43p, Rpc40p and Rsc8p, were present in this complex. Although its association with an H4-tail is not known, Rsc8p has a SANT domain, which was proposed as a histone tail interaction domain, as mentioned above.

Complex #3: The Nop58/Sik1 complex consists of three proteins, Nop58p, Sik1p and Nsr1p, which are all our candidate proteins. This complex is involved in ribosomal RNA (rRNA) processing and small nucleolar RNA (snoRNA)

synthesis (29). Whether the complex is associated with chromatin has not been investigated.

Complex #4: We found Arp2p, Rpc40p and Tif34p, which are included in the NTG1 complex (28). Ntg1p and Ntg2p, the *Saccharomyces cerevisiae* homologs of endonuclease III from *Escherichia coli*, are both required for the efficient repair of spontaneous or induced oxidative DNA damage in yeast (35). Although we did not investigate whether the NTG1 complex interacts with chromatin, recent reports have firmly established a mechanistic link between DNA repair and the recruitment of histone modifiers or ATP-dependent chromatin-remodeling complexes (36). A WD40-repeat within Tif34p may play a role in recruiting the NTG complex to chromatin.

Complex #5: The yTAP-C228 complex contains Fpr4p and Pwp1p (27). Fpr4p has both peptidyl propyl *cis-trans* isomerase activity and histone chaperone activity. Fpr4p is required for the *in vivo* silencing of the gene expression at a ribosomal DNA (rDNA) locus (37). Pwp1p, a protein with a WD40-repeat, is involved in rRNA processing and associates with *trans*-acting ribosome biogenesis factors (38). Thus, it is likely that the yTAP-C288 complex associates with the rDNA chromatin, and we will show that Pwp1p actually binds to the rDNA chromatin in an H4 tail-dependent manner (described below).

Complex #6: Both Rsc8p and YDL156Wp are components of the yTAP-C152 complex (27). This complex probably functions in DNA repair, since it includes many proteins (10 out of 35 components) involved in this process. Rsc8p may associate with a histone-tail by its SANT domain. YDL156Wp contains a WD40-repeat domain that shares 39% amino acid identity with that of the human Xeroderma pigmentosum group E (XP-E) protein p48 (also known as DDB2). p48 is a damage-specific DNA binding protein, and may play a role in repairing DNA lesions by associating with damaged chromatin via its WD40-repeat domain (39,40).

Complex #7: The general transcription factor TFIID has 15 subunits, including two candidates, Taf11p and Taf14p (41). The higher eukaryotic TAF1 has acetyltransferase activity, two bromodomains, and kinase activity. Its yeast homolog, Taf1p, has the acetyltransferase activity but lacks the bromodomains and the kinase activity. Bdf1p, like the higher eukaryotic TAF1, has the kinase activity located on the carboxyl-terminal side of its bromodomains. The structural and functional similarities suggest that Bdf1p corresponds to the carboxyl-terminal region of the higher eukaryotic TAF1 (42). The bromodomain of Bdf1p binds to an acetyllysine of the histone-tail (6,7). As shown in Figure 3B, we found that the amount of Bdf1p was lower in the oligomerized chromatin fraction from the H4-tail deleted cells. Thus, the amount of the TFIID complex associated with chromatin may be decreased in the H4-tail deleted cells.

Complex #8: Arp4p and Taf14p are components of both the NuA4 histone H4/H2A acetyltransferase and INO80 chromatin remodeling complexes (31,43). These complexes associate with chromatin through Arp4p (43,44).

Complex #9: Arp2p interacts with Srp1p both physically and genetically (45). Arp2p was shown to play an important role in nuclear pore complex structure and functions. Srp1, a karyopherin α , forms a heterodimer with Kap95p, a karyopherin β , to mediate the import of a nuclear protein

(46). Kap95p preferentially associates with a subset of highly transcribed genes (47). Active transcription is linked to an H4-tail modification, such as acetylation. It is likely that the complex containing Arp2p and Srp1p mediates the interaction between transcriptionally active chromatin and a nuclear pore complex.

Complex #10: The PKH1 complex (28), which is composed of four subunits, includes Lsp1p and Pil1p. They negatively regulate the 3-phosphoinositide-dependent protein kinase-like kinase Pkh1p and downstream signaling pathways (48). It is not known whether this complex interacts with chromatin. However, Pil1p is included in the yTAP-C7 complex, which was purified with TAP-tagged Scs2p (27). It is interesting that the deletion of *SCS2* reduced the silencing at telomeric chromatin, which is also caused by an H4-tail deletion (49).

As described above, our potential proteins, except for Cdc12p, are contained in one of the 10 complexes that may be involved in chromatin regulation. Of the 10 complexes, 3 are suggested to interact with the H4-tail by known tail-binding proteins and 5 have the potential for H4-tail binding activity by the proposed histone-tail associated domains: Arp4p in the #1 and #8 complexes, Isw1p in the #1 complex and Bdf1p in the #7 complex; a SANT domain of Rsc8 in the #1, #2 and #6 complexes, and WD40-repeat proteins in the #4, #5 and #6 complexes. In future experiments, we will investigate whether the H4-tail is required for chromatin association in each complex.

Pwp1p associates with chromatin at rDNA *in vivo* and its association is dependent on the H4-tail.

Our three candidate proteins, Pwp1p, Tif34p and YDL156Wp, share a WD40-repeat domain, which is present in many chromatin-associated factors. Several proteins containing the WD40-repeat have binding activity to a histone tail, and one of the several proteins, WDR5, binds to histone H3-tail via its WD40-repeat domain (described in Discussion). We focused on Pwp1p and constructed yeast strains in which the endogenous copy of the *PWP1* gene was modified to encode either 13 copies of a Myc epitope or 3 copies of a FLAG epitope at its C-terminus. *PWP1* is an essential gene, but neither tagged strain displayed a growth defect, indicating that the tagged proteins are functional. We investigated whether the amount of Pwp1p was reduced in the H4-tail deleted chromatin by a western blot analysis using Myc-tagged Pwp1p (Figure 5). Equal amounts of the oligomerized chromatin from both the WT and H4-tail Δ strains were fractionated on the gels and analyzed by western blotting with the anti-H3 and anti-H2A antibodies. The most appropriate loading control in this experiment is abundance of histone H4, which could be detected with the anti-H4 antibody against the C-terminus of histone H4. Unfortunately, we were not able to use histone H4 as the loading control, since the antibody gave the less signal intensity from the tail-deleted H4 than that from wild-type histone H4 in our western blot (data not shown). Chromatin consists of an equal amount of each core histone. The integrity of nucleosome is not altered in this H4-tail deleted strain (50). Therefore, we chose histone H3, instead of histone H4, as a loading

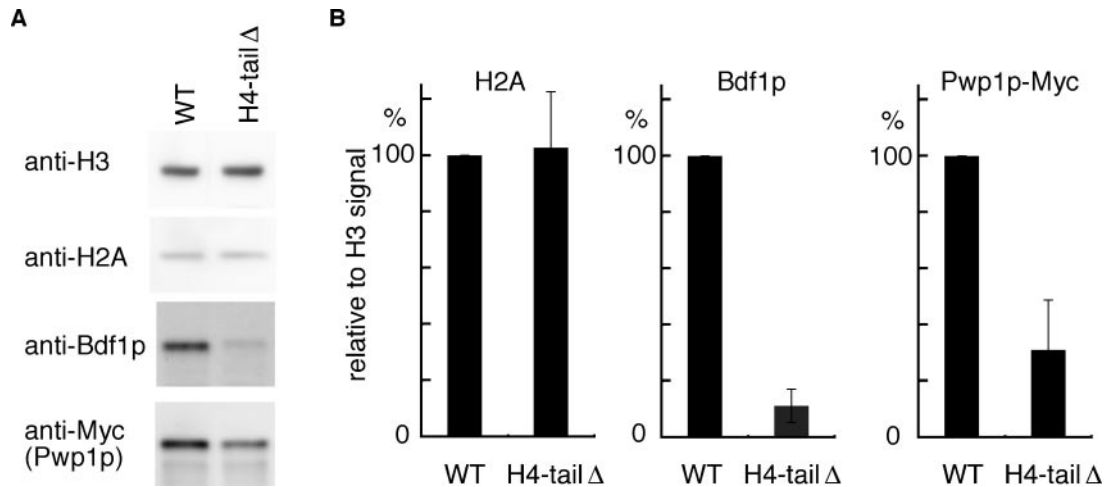


Figure 5. The amount of Pwp1p is reduced in H4 tail-deleted chromatin. (A) Western blot analyses were performed as in Figure 3B with Myc-tagged Pwp1p strains. (B) The graph shows the quantification of H2A, Bdf1p and Pwp1p-Myc relative to the H3 signal intensity. Data represent the average of five assays \pm SD.

control, whose amount represents the amount of chromatin. The amount of Pwp1p was decreased in the H4-tail deleted chromatin in a similar manner as Bdf1p, which has been shown to interact with the H4-tail (Figure 5A). The reductions of Bdf1p and Pwp1p were calculated to be 89 and 69%, respectively, when the signals were quantified in comparison with the histone H3 signal. On the other hand, the reduction of H2A was not observed (Figure 5A and 5B). The total amounts of Pwp1p in the cell were the same in the WT and H4-tail Δ strains (data not shown). Therefore, we concluded that the amount of Pwp1p in the oligomerized chromatin fraction is decreased by the H4-tail deletion.

Pwp1p is localized in the nucleolus and is involved in rRNA processing (38,51). However, how Pwp1p localizes to the nucleolus is unknown. The localization of Pwp1p to the nucleolus raised the possibility that Pwp1p may associate with the chromatin at rDNA. We assessed whether Pwp1p associates with the chromatin at rDNA by a ChrIP assay using the FLAG-tagged Pwp1p strain. To confirm our ChrIP assay using a FLAG-tagged protein, we investigated enrichment of FLAG-tagged Sir3p at silent chromatin. FLAG-tagged Sir3p is specifically recognized by an anti-FLAG antibody (data not shown). The immunoprecipitated DNA was quantified by multiplex PCR with primers for an *HMR* silent chromatin region, an *INO1* promoter region, and a loading control, a *CUP1* region (52). Our PCR amplifications were in the linear range (Figure 6A lanes 1–5). To calculate the relative fold enrichment of Sir3p binding to chromatin, we first normalized each signal to the *CUP1* loading control, and then compared its normalized signal with that of the input DNA used in each ChrIP assay. The fold enrichment values of an untagged strain indicated background binding. Consistent with the previous work (53), we found that Sir3p associates with the silent chromatin at the *HMR* region preferentially (3.1-fold), but not at the *INO1* region (Figure 6A lane 10 and 6B). We then used the anti-FLAG antibody to immunoprecipitate the FLAG-tagged Pwp1p-associated chromatin DNA. FLAG-tagged Pwp1p is specifically recognized by an anti-FLAG antibody (data not shown).

We examined the Pwp1p binding to a 9.1 kb rDNA repeat unit with 16 sets of primers that spanned the rDNA repeat unit (Figure 6E). The immunoprecipitated DNA was quantified by multiplex PCR with two sets of the primers for the rDNA regions and one set for the *CUP1* region (52). To calculate the relative fold enrichment of Pwp1p binding to the rDNA chromatin, we first normalized the rDNA regions to the *CUP1* region, and then compared its normalized signal with that of input DNA. We generated a graphical representation of Pwp1p association across the rDNA repeat using the relative fold enrichment values for each DNA fragment (Figure 6E, closed circles). The fold enrichment values of the untagged strain indicated background binding (Figure 6E open circles). We found that Pwp1p only associated with a 5' region of 25S rDNA, not at other regions. The ChrIP data used to obtain the graph at 3.1 kb (25S) and 8.1 kb (5S) positions and the linear amplification of the PCR is shown in Figure 6C and 6D. We found that the immunoprecipitated DNA from the 25S rDNA region was enriched \sim 5.5-fold in the FLAG-tagged strain. In contrast, the immunoprecipitated DNA from the 5S rDNA and the *INO1* regions were not significantly enriched in the FLAG-tagged strain (Figure 6C and 6D for the 5S rDNA region and Figure 6A and 6B for the *INO1* region). These results indicated that Pwp1p binds preferentially to the chromatin at the 25S rDNA region.

We next investigated whether the Pwp1p binding to the 25S rDNA chromatin is dependent on the H4-tail. As shown in Figure 6C–E, no enrichment was observed at the 25S rDNA regions in the FLAG-tagged H4-tail Δ strain. Quantification showed that the fold enrichment of the Pwp1p binding to the 25S rDNA region in the FLAG-tagged and the untagged H4-tail Δ strains was 2.6-fold and 1.7-fold, respectively (Figure 6D). These results demonstrated that the level of the Pwp1p binding at the 25S regions in the H4-tail Δ strain is much reduced compared to that in the WT strain. Thus, we obtained *in vivo* evidence that Pwp1p associates with the 25S rDNA chromatin and its association is dependent on the N-terminal-tail of histone H4.

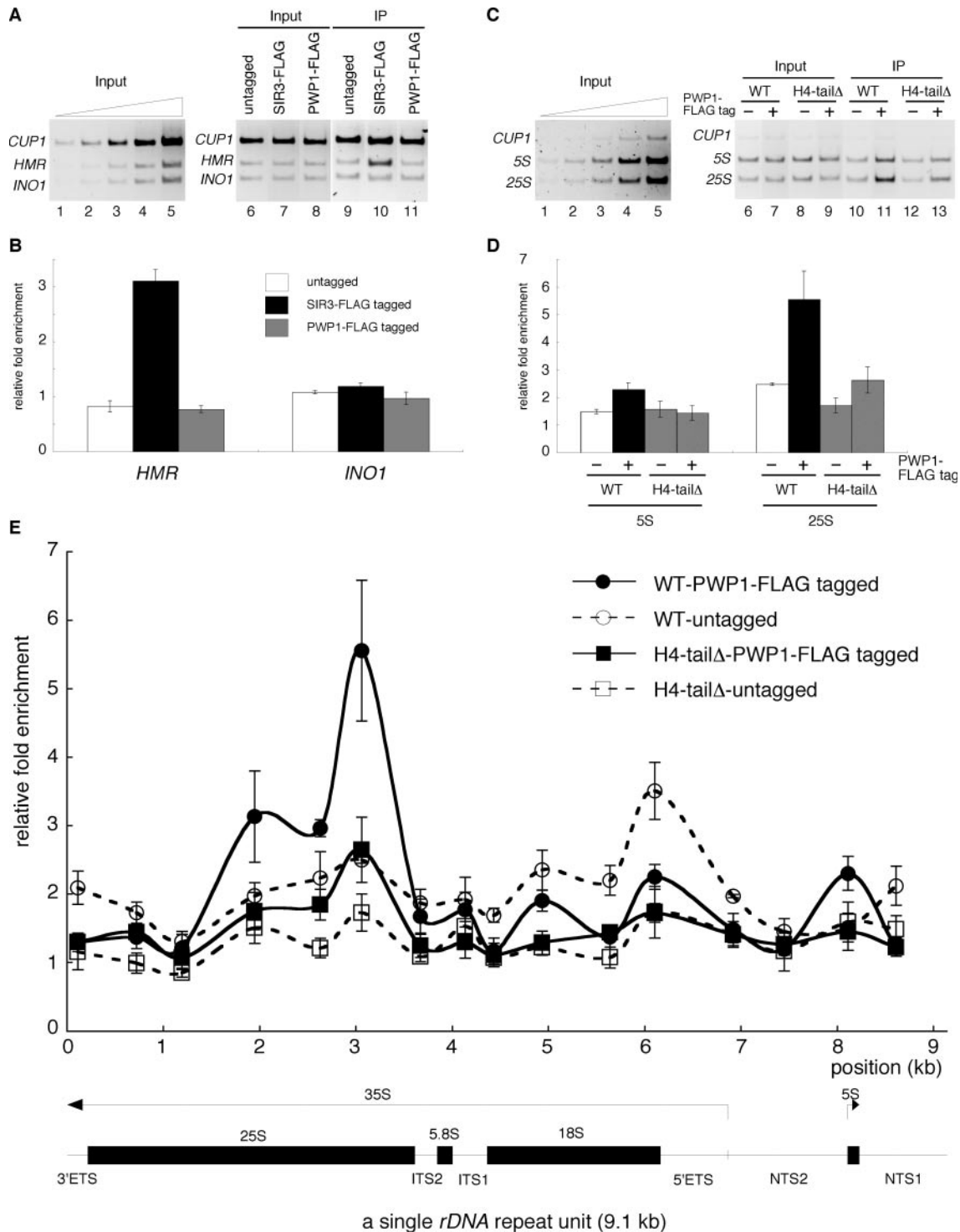


Figure 6. Pwp1p associates with the rDNA chromatin in an H4-tail-dependent manner. (A) ChrIP assays were performed with the cells containing the FLAG-tagged Sir3p, the FLAG-tagged Pwp1p and untagged proteins. Serial 2.5-fold dilutions of input DNA and the immunoprecipitated DNA were analyzed by multiplex PCR using primer pairs directed against the *CUP1*, *HMR*, and *INO1* loci. (B) The bar graphs show the relative fold enrichment of the FLAG-tagged Sir3p, the FLAG-tagged Pwp1p and the untagged protein at the *HMR* and the *INO1* loci. Data represent the average of three assays \pm SD. (C) ChrIP assays were performed with the FLAG-tagged and the untagged Pwp1ps in the WT and H4-tail Δ cells. Serial 2.5-fold dilutions of input DNA and the immunoprecipitated DNA were analyzed by multiplex PCR using primer pairs directed against the *CUP1*, the 5S (at 8.1 kb in E) and the 25S (at 3.1 kb in E) loci. (D) The bar graphs show the relative fold enrichment of the Pwp1p binding at the 5S and 25S loci in (C). Data represent the average of three assays \pm SD. (E) ChrIP assays were performed as shown in (C) using 16 sets of primers that spanned the rDNA repeat unit. The graph shows the relative fold enrichment of the Pwp1p binding across an rDNA repeat unit, which is schematically indicated under the X-axis. Each repeat yields a Pol I-transcribed 35S precursor rRNA (shown as an arrow with 35S) and a pol III-transcribed 5S rRNA (shown as an arrow with 5S). The repeat contains the genes for 5S, 5.8S, 18S and 25S rRNAs (black boxes), as well as three types of spacer regions: internal transcribed spacers (ITS1, ITS2), external transcribed spacers (5' ETS, 3' ETS) and non-transcribed spacers (NTS1, NTS2). Data represent the average of three assays \pm SD.

DISCUSSION

We performed the protein differential display approach in 2DGE with the H4-tail deleted mutant to identify the H4-tail-associated-proteins by MS and identified 22 candidate proteins, including the H4-tail binding proteins, Arp4p and Isw1p, and proteins with the SANT and WD40-repeat, which may be a histone tail-binding domain. We also provided *in vivo* evidence that one candidate, Pwp1p, associates with the rDNA chromatin in an H4 tail-dependent manner.

In previous reports, in order to identify protein complexes capable of binding specifically to histone H3 N-terminal tail, nuclear extracts were applied to affinity columns displaying either unmodified H3 tails or the same tails but differently methylated at specific residues. The NuRD complex binds specifically to unmodified H3 tails but not to K4 methylated tails (14). Two proteins, INHAT complex subunits SET and pp32, bind specifically to unmodified H3 tails but not to phosphorylated tails at T3 (16). hSNF2H and WDR5 were identified as H3 tail-binding proteins that associate with the methylated tail at K4 (15,17). The 14-3-3 isoforms also bind to the phosphorylated H3-tail at S10 (18). These protein identifications proved that the peptide affinity column is a powerful method to identify the tail-binding proteins. However, this approach is dependent on the preparation of a nuclear extract and the salt concentration of the binding buffer. Most importantly, the peptide conformation could be different from that in the chromatin context *in vivo*. Thus, the screening may be restricted, and some proteins would not be identified. By a yeast two-hybrid screen employing yeast genomic libraries in combination with a bait plasmid expressing a fragment of histone H4 (amino acids 1–59), only two proteins, Bdf1p and Hif1p, were identified (54,55). This indicates that the two-hybrid screen also has limitations. The authors suggested that a folding difference may exist between the full-length histone H4 and the portion of amino acids 1–59 (54). Again, the tail in this assay may have a different conformation as compared to that in the chromatin context. In this regard, our approach seems to be more suitable than the others to identify tail-binding proteins. The nucleosome ladder was detected by MNase digestion in our H4-tail mutant, showing the maintenance of the nucleosome structure in the absence of H4-tails (50 and data not shown). Therefore, our screening reflects the H4-tail binding ability *in vivo*.

We enriched chromatin proteins by the Mg^{2+} -dependent oligomerization for an efficient identification of a histone-tail binding protein (Figure 2). However, silver stained 2D gels were not sensitive enough to identify Sir3p, whose abundance was reduced in western blot (Figure 3B). Total mixture mass spectrometry is more sensitive than the silver stain. This method will help to identify less-abundant proteins.

Our screening is based on *in vivo* binding activity. So a candidate protein may interact either directly or indirectly with an H4-tail. We identified Isw1p, whose fly homolog, ISWI, probably recognizes a DNA-bound H4-tail. ISWI does not interact stably with the GST–H4 tail fusion protein in the absence of DNA (32). This type of a binding protein cannot be identified by a widely used approach such as the peptide affinity column.

Histone tails are involved in folding higher-order chromatin structures (2). In the tail mutant strain, the chromatin structures may be altered at the higher-order folding level. The MNase digestion produced a nucleosomal ladder in the H4-tail Δ , and its MNase sensitivity was higher than that of the WT, suggesting a structural alteration beyond the nucleosomal level by the tail-deletion (50). If there is a protein that recognizes the higher-order chromatin structure, then the amount of this protein would also be decreased in our screening. Such a protein may be included among our candidate proteins. We cannot examine this possibility at present, as there is no biochemical method to assess the folding of higher-order chromatin *in vivo*.

The WD40-repeat is defined by a sequence repeat of ~ 40 amino acids, typically beginning with a glycine–histidine pair and ending with a tryptophan–aspartic acid pair. This motif is shared among over 30 functional families, which are involved in signal transduction, mRNA synthesis, RNA splicing, vascular trafficking, cytoskeletal assembly, control of transcription initiation complex assembly and a chromatin-regulated complex (56). Among the chromatin-regulated proteins, several WD40-repeat proteins are known as histone-tail binding proteins. For example, the transcriptional repressor proteins Tup1p, Groucho and transducin beta-like protein (TBL1)/TBL1-related protein (TBLR1) associate with a histone-tail via a domain other than the WD40-repeat domain (57–59). WDR5, a common component of three H3 K4 methyltransferase complexes (the mixed-lineage leukemia gene (MLL)1, MLL2 and hSet1), directly associates with a histone H3-tail di- and trimethylated at K4 via the WD40-repeat domain itself (17). We plan to investigate whether the three candidates (Pwp1p, Tif34p, and YDL156Wp) interact with the H4-tail directly or indirectly.

rDNA transcription accounts for $\sim 60\%$ of the transcription in a rapidly growing yeast cell. However, only about half of the ~ 150 copies of the rDNA are active at any given time, whereas the remaining copies are maintained in a silenced state. This ratio of active to inactive genes is stably propagated throughout the cell cycle and is independent of the transcriptional activity of the cell. The regulatory mechanism that controls the ratio of active to inactive rDNA genes is poorly understood, but rDNA silencing is one of the factors that establish and maintain the transcriptionally inactive rDNA genes. We showed that Pwp1p associates with the rDNA chromatin, and its association is dependent on the H4-tail. The importance of the H4-tail for rDNA regulation was also suggested by studies of a mammalian nucleolar remodeling complex (NoRC) and a yeast regulator of nucleolar silencing and telophase exit (RENT) complex, which both regulate rDNA silencing. The NoRC induces nucleosome sliding in an ATP- and histone H4 tail-dependent fashion, and the NoRC-directed rDNA repression requires the histone H4-tail (60,61). The RENT complex mediates the rDNA silencing and deacetylates the acetylated K16 of the H4-tail by Sir2p (52,62–64). These studies raised the possibility that the H4-tail binding protein that associates with the rDNA chromatin performs a role similar to that of Sir3p in the silencing at telomeric and HM loci. Pwp1p may be the factor that links the RENT complex to the rDNA chromatin through the H4-tail.

The yTAP-C288 complex consists of eight subunits: Act1p, Eno2p, Fpr4p, Nan1p, Pol5p, Pwp1p, Smc1p and YPL207Wp (27). Other subunits besides Pwp1p may also function in the rDNA regulation. For instance, Fpr4p binds to rDNA chromatin and regulates rDNA silencing (37); Nan1p associates with the RENT complex (63) and Pol5p is required for the synthesis of rRNA (65). In addition, Smc1p is a member of a ubiquitous family of chromosome-associated ATPases and plays a role in chromosome dynamics (66). Taken together, we propose that the yTAP-C288 complex associates with rDNA chromatin by the histone H4-tail and regulates rDNA transcription by modulating the chromatin structure.

We compared the Mg²⁺-dependent oligomerized chromatins isolated from H4 tail deletion cells and wild type cells by the protein differential display approach in 2DGE, and effectively identified histone-tail binding proteins. Other tail-deleted and point mutant cells are possible sources for the identification of tail-binding proteins for other core histones and specifically modified histones, respectively.

ACKNOWLEDGEMENTS

The authors are grateful to Michael Grunstein for the histone-tail-mutant strain, Toshio Tsukiyama for the p3FLAG-KanMX plasmid, Mark Longtine for the pFA6a-13Myc-TRP1 plasmid, and Shirleen G. Roeder for the anti-BDF1 antibody. This work was supported by a research grant endorsed by the New Energy and Industrial Technology Development Organization (NEDO) and by Grants-in-Aid from the Ministry of Education, Science, Sports and Culture of Japan (MEXT). Funding to pay the Open Access publication charges for this article was provided by MEXT.

Conflict of interest statement. None declared.

REFERENCES

- Luger,K., Mader,A.W., Richmond,R.K., Sargent,D.F. and Richmond,T.J. (1997) Crystal structure of the nucleosome core particle at 2.8 Å resolution. *Nature*, **389**, 251–260.
- Hansen,J.C. (2002) Conformational dynamics of the chromatin fiber in solution: determinants, mechanisms, and functions. *Annu. Rev. Biophys. Biomol. Struct.*, **31**, 361–392.
- Zheng,C., Lu,X., Hansen,J.C. and Hayes,J.J. (2005) Salt-dependent intra- and internucleosomal interactions of the H3 tail domain in a model oligonucleosomal array. *J. Biol. Chem.*, **280**, 33552–33557.
- Hecht,A., Laroche,T., Strahl-Bolsinger,S., Gasser,S.M. and Grunstein,M. (1995) Histone H3 and H4 N-termini interact with SIR3 and SIR4 proteins: a molecular model for the formation of heterochromatin in yeast. *Cell*, **80**, 583–592.
- Carmen,A.A., Milne,L. and Grunstein,M. (2002) Acetylation of the yeast histone H4 N terminus regulates its binding to heterochromatin protein SIR3. *J. Biol. Chem.*, **277**, 4778–4781.
- Matangkasombut,O. and Buratowski,S. (2003) Different sensitivities of bromodomain factors 1 and 2 to histone H4 acetylation. *Mol. Cell*, **11**, 353–363.
- Ladurner,A.G., Inouye,C., Jain,R. and Tjian,R. (2003) Bromodomains mediate an acetyl-histone encoded antisilencing function at heterochromatin boundaries. *Mol. Cell*, **11**, 365–376.
- Kimura,A., Umehara,T. and Horikoshi,M. (2002) Chromosomal gradient of histone acetylation established by Sas2p and Sir2p functions as a shield against gene silencing. *Nat. Genet.*, **32**, 370–377.
- Suka,N., Luo,K. and Grunstein,M. (2002) Sir2p and Sas2p oppositely regulate acetylation of yeast histone H4 lysine16 and spreading of heterochromatin. *Nat. Genet.*, **32**, 378–383.
- Lachner,M., O'Carroll,D., Rea,S., Mechtler,K. and Jenuwein,T. (2001) Methylation of histone H3 lysine 9 creates a binding site for HP1 proteins. *Nature*, **410**, 116–120.
- Bannister,A.J., Zegerman,P., Partridge,J.F., Miska,E.A., Thomas,J.O., Allshire,R.C. and Kouzarides,T. (2001) Selective recognition of methylated lysine 9 on histone H3 by the HP1 chromo domain. *Nature*, **410**, 120–124.
- Cao,R., Wang,L., Wang,H., Xia,L., Erdjument-Bromage,H., Tempst,P., Jones,R.S. and Zhang,Y. (2002) Role of histone H3 lysine 27 methylation in Polycomb-group silencing. *Science*, **298**, 1039–1043.
- Jenuwein,T. and Allis,C.D. (2001) Translating the histone code. *Science*, **293**, 1074–1080.
- Zegerman,P., Canas,B., Pappin,D. and Kouzarides,T. (2002) Histone H3 lysine 4 methylation disrupts binding of nucleosome remodeling and deacetylase (NuRD) repressor complex. *J. Biol. Chem.*, **277**, 11621–11624.
- Santos-Rosa,H., Schneider,R., Bernstein,B.E., Karabetsou,N., Morillon,A., Weise,C., Schreiber,S.L., Mellor,J. and Kouzarides,T. (2003) Methylation of histone H3 K4 mediates association of the Isw1p ATPase with chromatin. *Mol. Cell*, **12**, 1325–1332.
- Schneider,R., Bannister,A.J., Weise,C. and Kouzarides,T. (2004) Direct binding of INHAT to H3 tails disrupted by modifications. *J. Biol. Chem.*, **279**, 23859–23862.
- Wysocka,J., Swigut,T., Milne,T.A., Dou,Y., Zhang,X., Burlingame,A.L., Roeder,R.G., Brivanlou,A.H. and Allis,C.D. (2005) WDR5 associates with histone H3 methylated at K4 and is essential for H3 K4 methylation and vertebrate development. *Cell*, **121**, 859–872.
- Macdonald,N., Welburn,J.P., Noble,M.E., Nguyen,A., Yaffe,M.B., Clynes,D., Moggs,J.G., Orphanides,G., Thomson,S., Edmunds,J.W. *et al.* (2005) Molecular basis for the recognition of phosphorylated and phosphoacetylated histone H3 by 14-3-3. *Mol. Cell*, **20**, 199–211.
- Durrin,L.K., Mann,R.K., Kayne,P.S. and Grunstein,M. (1991) Yeast histone H4 N-terminal sequence is required for promoter activation *in vivo*. *Cell*, **65**, 1023–1031.
- Gelbart,M.E., Rechsteiner,T., Richmond,T.J. and Tsukiyama,T. (2001) Interactions of Isw2 chromatin remodeling complex with nucleosomal arrays: analyses using recombinant yeast histones and immobilized templates. *Mol. Cell Biol.*, **21**, 2098–2106.
- Longtine,M.S., McKenzie,A., III, Demarini,D.J., Shah,N.G., Wach,A., Brachat,A., Philippsen,P. and Pringle,J.R. (1998) Additional modules for versatile and economical PCR-based gene deletion and modification in *Saccharomyces cerevisiae*. *Yeast*, **14**, 953–961.
- Liang,C. and Stillman,B. (1997) Persistent initiation of DNA replication and chromatin-bound MCM proteins during the cell cycle in *cdc6* mutants. *Genes Dev.*, **11**, 3375–3386.
- Alfieri,J.A. and Clark,D.J. (1999) Isolation of minichromosomes from yeast cells. *Methods Enzymol.*, **304**, 35–49.
- Suka,N., Suka,Y., Carmen,A.A., Wu,J. and Grunstein,M. (2001) Highly specific antibodies determine histone acetylation site usage in yeast heterochromatin and euchromatin. *Mol. Cell*, **8**, 473–479.
- Goldmark,J.P., Fazio,T.G., Estep,P.W., Church,G.M. and Tsukiyama,T. (2000) The Isw2 chromatin remodeling complex represses early meiotic genes upon recruitment by Ume6p. *Cell*, **103**, 423–433.
- Schwarz,P.M., Felthauer,A., Fletcher,T.M. and Hansen,J.C. (1996) Reversible oligonucleosome self-association: dependence on divalent cations and core histone tail domains. *Biochemistry*, **35**, 4009–4015.
- Gavin,A.C., Bosche,M., Krause,R., Grandi,P., Marzioch,M., Bauer,A., Schultz,J., Rick,J.M., Michon,A.M., Cruciat,C.M. *et al.* (2002) Functional organization of the yeast proteome by systematic analysis of protein complexes. *Nature*, **415**, 141–147.
- Ho,Y., Gruhler,A., Heilbut,A., Bader,G.D., Moore,L., Adams,S.L., Millar,A., Taylor,P., Bennett,K., Boutilier,K. *et al.* (2002) Systematic identification of protein complexes in *Saccharomyces cerevisiae* by mass spectrometry. *Nature*, **415**, 180–183.
- Krogan,N.J., Peng,W.T., Cagney,G., Robinson,M.D., Haw,R., Zhong,G., Guo,X., Zhang,X., Canadien,V., Richards,D.P. *et al.* (2004) High-definition macromolecular composition of yeast RNA-processing complexes. *Mol. Cell*, **13**, 225–239.
- Harata,M., Oma,Y., Mizuno,S., Jiang,Y.W., Stillman,D.J. and Wintersberger,U. (1999) The nuclear actin-related protein of *Saccharomyces cerevisiae*, Act3p/Arp4, interacts with core histones. *Mol. Biol. Cell*, **10**, 2595–2605.

31. Galarneau, L., Nourani, A., Boudreault, A.A., Zhang, Y., Heliot, L., Allard, S., Savard, J., Lane, W.S., Stillman, D.J. and Cote, J. (2000) Multiple links between the NuA4 histone acetyltransferase complex and epigenetic control of transcription. *Mol. Cell*, **5**, 927–937.
32. Clapier, C.R., Nightingale, K.P. and Becker, P.B. (2002) A critical epitope for substrate recognition by the nucleosome remodeling ATPase ISWI. *Nucleic Acids Res.*, **30**, 649–655.
33. Boyer, L.A., Latek, R.R. and Peterson, C.L. (2004) The SANT domain: a unique histone-tail-binding module? *Nat. Rev. Mol. Cell Biol.*, **5**, 158–163.
34. Mellor, J. and Morillon, A. (2004) ISWI complexes in *Saccharomyces cerevisiae*. *Biochim. Biophys. Acta*, **1677**, 100–112.
35. Hanna, M., Chow, B.L., Morey, N.J., Jinks-Robertson, S., Doetsch, P.W. and Xiao, W. (2004) Involvement of two endonuclease III homologs in the base excision repair pathway for the processing of DNA alkylation damage in *Saccharomyces cerevisiae*. *DNA Repair (Amst)*, **3**, 51–59.
36. van Attikum, H. and Gasser, S.M. (2005) The histone code at DNA breaks: a guide to repair? *Nat. Rev. Mol. Cell Biol.*, **6**, 757–765.
37. Kuzuhara, T. and Horikoshi, M. (2004) A nuclear FK506-binding protein is a histone chaperone regulating rDNA silencing. *Nat. Struct. Mol. Biol.*, **11**, 275–283.
38. Zhang, W., Morris, Q.D., Chang, R., Shai, O., Bakowski, M.A., Mitsakakis, N., Mohammad, N., Robinson, M.D., Zirngibl, R., Somogyi, E. et al. (2004) The functional landscape of mouse gene expression. *J. Biol.*, **3**, 21.
39. Ropic-Otrin, V., Navazza, V., Nardo, T., Botta, E., McLenigan, M., Bisi, D.C., Levine, A.S. and Stefanini, M. (2003) True XP group E patients have a defective UV-damaged DNA binding protein complex and mutations in DDB2 which reveal the functional domains of its p48 product. *Hum. Mol. Genet.*, **12**, 1507–1522.
40. Hwang, B.J., Toering, S., Francke, U. and Chu, G. (1998) p48 Activates a UV-damaged-DNA binding factor and is defective in xeroderma pigmentosum group E cells that lack binding activity. *Mol. Cell. Biol.*, **18**, 4391–4399.
41. Sanders, S.L. and Weil, P.A. (2000) Identification of two novel TAF subunits of the yeast *Saccharomyces cerevisiae* TFIID complex. *J. Biol. Chem.*, **275**, 13895–13900.
42. Matangkasombut, O., Buratowski, R.M., Swilling, N.W. and Buratowski, S. (2000) Bromodomain factor I corresponds to a missing piece of yeast TFIID. *Genes Dev.*, **14**, 951–962.
43. Shen, X., Ranallo, R., Choi, E. and Wu, C. (2003) Involvement of actin-related proteins in ATP-dependent chromatin remodeling. *Mol. Cell*, **12**, 147–155.
44. Downs, J.A., Allard, S., Jobin-Robitaille, O., Javaheri, A., Auger, A., Bouchard, N., Kron, S.J., Jackson, S.P. and Cote, J. (2004) Binding of chromatin-modifying activities to phosphorylated histone H2A at DNA damage sites. *Mol. Cell*, **16**, 979–990.
45. Yan, C., Leibowitz, N. and Melese, T. (1997) A role for the divergent actin gene, ACT2, in nuclear pore structure and function. *EMBO J.*, **16**, 3572–3586.
46. Enenkel, C., Blobel, G. and Rexach, M. (1995) Identification of a yeast karyopherin heterodimer that targets import substrate to mammalian nuclear pore complexes. *J. Biol. Chem.*, **270**, 16499–16502.
47. Casolari, J.M., Brown, C.R., Komili, S., West, J., Hieronymus, H. and Silver, P.A. (2004) Genome-wide localization of the nuclear transport machinery couples transcriptional status and nuclear organization. *Cell*, **117**, 427–439.
48. Zhang, X., Lester, R.L. and Dickson, R.C. (2004) Pil1p and Lsp1p negatively regulate the 3-phosphoinositide-dependent protein kinase-like kinase Pkh1p and downstream signaling pathways Pkc1p and Ypk1p. *J. Biol. Chem.*, **279**, 22030–22038.
49. Craven, R.J. and Petes, T.D. (2001) The *Saccharomyces cerevisiae* suppressor of choline sensitivity (*SCS2*) gene is a multicopy suppressor of *mecl* telomeric silencing defects. *Genetics*, **158**, 145–154.
50. Kayne, P.S., Kim, U.J., Han, M., Mullen, J.R., Yoshizaki, F. and Grunstein, M. (1988) Extremely conserved histone H4 N terminus is dispensable for growth but essential for repressing the silent mating loci in yeast. *Cell*, **55**, 27–39.
51. Huh, W.K., Falvo, J.V., Gerke, L.C., Carroll, A.S., Howson, R.W., Weissman, J.S. and O'Shea, E.K. (2003) Global analysis of protein localization in budding yeast. *Nature*, **425**, 686–691.
52. Huang, J. and Moazed, D. (2003) Association of the RENT complex with nontranscribed and coding regions of rDNA and a regional requirement for the replication fork block protein Fob1 in rDNA silencing. *Genes Dev.*, **17**, 2162–2176.
53. Hecht, A., Strahl-Bolsinger, S. and Grunstein, M. (1996) Spreading of transcriptional repressor SIR3 from telomeric heterochromatin. *Nature*, **383**, 92–96.
54. Pamblanco, M., Poveda, A., Sendra, R., Rodriguez-Navarro, S., Perez-Ortin, J.E. and Tordera, V. (2001) Bromodomain factor I (Bdf1) protein interacts with histones. *FEBS Lett.*, **496**, 31–35.
55. Poveda, A., Pamblanco, M., Tafrov, S., Tordera, V., Sternglanz, R. and Sendra, R. (2004) Hif1 is a component of yeast histone acetyltransferase B, a complex mainly localized in the nucleus. *J. Biol. Chem.*, **279**, 6033–6043.
56. Yu, L., Gaitatzes, C., Neer, E. and Smith, T.F. (2000) Thirty-plus functional families from a single motif. *Protein Sci.*, **9**, 2470–2476.
57. Edmondson, D.G., Smith, M.M. and Roth, S.Y. (1996) Repression domain of the yeast global repressor Tup1 interacts directly with histones H3 and H4. *Genes Dev.*, **10**, 1247–1259.
58. Palaparti, A., Baratz, A. and Stifani, S. (1997) The Groucho/transducin-like enhancer of split transcriptional repressors interact with the genetically defined amino-terminal silencing domain of histone H3. *J. Biol. Chem.*, **272**, 26604–26610.
59. Yoon, H.G., Chan, D.W., Huang, Z.Q., Li, J., Fondell, J.D., Qin, J. and Wong, J. (2003) Purification and functional characterization of the human N-CoR complex: the roles of HDAC3, TBL1 and TBLR1. *EMBO J.*, **22**, 1336–1346.
60. Strohner, R., Nemeth, A., Jansa, P., Hofmann-Rohrer, U., Santoro, R., Langst, G. and Grummt, I. (2001) NoRC—a novel member of mammalian ISWI-containing chromatin remodeling machines. *EMBO J.*, **20**, 4892–4900.
61. Zhou, Y. and Grummt, I. (2005) The PHD finger/bromodomain of NoRC interacts with acetylated histone H4K16 and is sufficient for rDNA silencing. *Curr. Biol.*, **15**, 1434–1438.
62. Straight, A.F., Shou, W., Dowd, G.J., Turck, C.W., Deshaies, R.J., Johnson, A.D. and Moazed, D. (1999) Net1, a Sir2-associated nucleolar protein required for rDNA silencing and nucleolar integrity. *Cell*, **97**, 245–256.
63. Shou, W., Seol, J.H., Shevchenko, A., Baskerville, C., Moazed, D., Chen, Z.W., Jang, J., Shevchenko, A., Charbonneau, H. and Deshaies, R.J. (1999) Exit from mitosis is triggered by Tem1-dependent release of the protein phosphatase Cdc14 from nucleolar RENT complex. *Cell*, **97**, 233–244.
64. Tanny, J.C., Kirkpatrick, D.S., Gerber, S.A., Gygi, S.P. and Moazed, D. (2004) Budding yeast silencing complexes and regulation of Sir2 activity by protein-protein interactions. *Mol. Cell Biol.*, **24**, 6931–6946.
65. Shimizu, K., Kawasaki, Y., Hiraga, S., Tawaramoto, M., Nakashima, N. and Sugino, A. (2002) The fifth essential DNA polymerase phi in *Saccharomyces cerevisiae* is localized to the nucleolus and plays an important role in synthesis of rRNA. *Proc. Natl. Acad. Sci. USA*, **99**, 9133–9138.
66. Hirano, T. (2000) Chromosome cohesion, condensation, and separation. *Annu. Rev. Biochem.*, **69**, 115–144.